2012

Late-Stage Maturation of the Rieske Fe/S Protein: Mzm1 Stabilizes Rip1 but Does Not Facilitate Its Translocation by the AAA ATPase Bcs1

Tie-Zhong Cui
University of Utah Health Sciences Center

Pamela M. Smith
University of Utah Health Sciences Center

Jennifer L. Fox
University of Utah Health Sciences Center

Oleh Khalimonchuk
University of Nebraska-Lincoln, okhalimonchuk2@unl.edu

Dennis R. Winge
University of Utah Health Sciences Center

PMCID: PMC3486142

Late-Stage Maturation of the Rieske Fe/S Protein: Mzm1 Stabilizes Rip1 but Does Not Facilitate Its Translocation by the AAA ATPase Bcs1

Tie-Zhong Cui, Pamela M. Smith, Jennifer L. Fox,* Oleh Khalimonchuk,* and Dennis R. Winge

University of Utah Health Sciences Center, Departments of Medicine and Biochemistry, Salt Lake City, Utah, USA

The final step in the assembly of the ubiquinol-cytochrome *c* reductase or bc_1 complex involves the insertion of the Rieske Fe/S cluster protein, Rip1. Maturation of Rip1 occurs within the mitochondrial matrix prior to its translocation across the inner membrane (IM) in a process mediated by the Bcs1 ATPase and subsequent insertion into the bc_1 complex. Here we show that the matrix protein Mzm1 functions as a Rip1 chaperone, stabilizing Rip1 prior to the translocation step. In the absence of Mzm1, Rip1 is prone to either proteolytic degradation or temperature-induced aggregation. A series of Rip1 truncations were engineered to probe motifs necessary for Mzm1 interaction and Bcs1-mediated translocation of Rip1. The Mzm1 interaction with Rip1 persists in Rip1 variants lacking its transmembrane domain or containing only its C-terminal globular Fe/S domain. Replacement of the globular domain of Rip1 with that of the heterologous folded protein Grx3 abrogated Mzm1 interaction; however, appending the C-terminal 30 residues of Rip1 to the Rip1-Grx3 chimera restored Mzm1 interaction. The Rip1-Grx3 chimera and a Rip1 truncation containing only the N-terminal 92 residues each induced stabilization of the bc_1:cytochrome oxidase supercomplex in a Bcs1-dependent manner. However, the Rip1 variants were not stably associated with the supercomplex. The induced supercomplex stabilization by the Rip1 N terminus was independent of Mzm1.

The ubiquinol-cytochrome *c* reductase (bc_1 complex, complex III) is a key component of the mitochondrial electron transfer chain involved in oxidative phosphorylation. The enzyme mediates the oxidation of ubiquinol and reduction of cytochrome *c*. This electron transfer step is coupled to proton translocation across the mitochondrial inner membrane (IM), creating the proton gradient used for ATP synthesis. The eukaryotic bc_1 complex exists as a dimeric unit consisting of 10 to 11 subunits, three of which contain the redox cofactors forming the catalytic center (17, 30). In contrast, the bacterial complex contains the core redox subunits and a single supernumerary subunit, if any (13). One core redox subunit, cytochrome *b* (Cob), is encoded by the mitochondrial DNA, while all other subunits are encoded by the nuclear genome and imported into the organelle. The other catalytic subunits are the Rieske protein (Rip1) with a 2Fe-2S center and the cytochrome c_1 protein (Cyt1). The Rieske Fe/S protein is intertwined between adjacent monomers of the bc_1 complex, with its globular domain in one unit and its transmembrane helix in the adjacent unit (17, 30). In addition to the stabilization imparted by Rip1, the dimeric bc_1 complex is also stabilized by interactions of the Cob subunits and the matrix-facing Cor2 subunits (17, 30). The dimeric bc_1 complex forms higher-order supercomplexes with cytochrome *c* oxidase (CcO, complex IV) in *Saccharomyces cerevisiae* and with both CcO and NADH dehydrogenase (complex I) in metazoans (23, 25).

Biogenesis of the bc_1 complex occurs in a modular assembly pathway with the mitochondrial Cob subunit seeding the assembly process (31, 32). An early core complex that contains Cob along with two small subunits, Qcr7 and Qcr8, is documented in yeast (7, 32). Addition of the subunits Cyt1, Cor1, Cor2, and Qcr6 leads to a late core assembly intermediate, which stably accumulates in yeast that are stalled in late steps of bc_1 complex maturation, including cells lacking Rip1 or the Bcs1 assembly factor (7, 9, 31). Since Rip1 contains the essential 2Fe-2S center that mediates electron transfer to the cytochrome c_1 subunit Cyt1, the late core intermediate is devoid of function. Qcr10 is a late addition with Rip1 (9, 31), which appears to stabilize the final complex (4) that associates with CcO to form supercomplex assemblies (8, 12, 31). The bc_1:CcO supercomplexes are destabilized in cells lacking Rip1 (8, 30), so the addition of Rip1 and Qcr10 appears to stabilize the supercomplexes.

Rip1 maturation involves a series of processing and translocation steps. Initially, a precursor form of Rip1 is imported across the mitochondrial IM into the matrix by the TIM23 translocase complex. The mature polypeptide is then generated by cleavage of the mitochondrial targeting sequence (MTS) and, in *Saccharomyces cerevisiae*, by a second cleavage of an N-terminal octapeptide (14, 16, 24). The MTS of yeast Rip1 consists of the N-terminal 22 residues, so upon both processing steps the mature Rip1 consists of residues 31 to 215 (20). Insertion of the 2Fe-2S center into the C-terminal globular domain likely occurs within the matrix by the ISC Fe-S cluster system (18). Insertion of this holo-Rip1 into the bc_1 late core intermediate requires a second translocation step in which this C-terminal domain is exposed to the intermem-

Received 2 April 2012 **Returned for modification** 14 June 2012
Accepted 20 August 2012
Published ahead of print 27 August 2012

Address correspondence to Dennis R. Winge, dennis.winge@hsc.utah.edu.

* Present address: Oleh Khalimonchuk, Department of Biochemistry and Redox Biology Center, University of Nebraska—Lincoln, Lincoln, Nebraska, USA; Jennifer L. Fox, Department of Chemistry and Biochemistry, College of Charleston, Charleston, South Carolina, USA.

T.-Z.C. and P.M.S. contributed equally to this work.

doi:10.1128/MCB.00441-12

brane space (IMS) side of the IM, to which it remains accessible after installation into the bc_1 complex. This second translocation step of Rip1 involves a folded domain, the Fe/S-containing C-terminal globular domain, which is moved across the IM. Whereas bacteria accomplish this translocation by the Tat translocase (3), eukaryotes use an AAA ATPase, Bcs1, for this step (27). Bcs1 associates with the late core assembly intermediate and mediates Rip1 translocation and insertion into the bc_1 complex (27). Cells lacking Bcs1 resemble *rip1*Δ or *qcr9*Δ cells in forming a stable, stalled, late core intermediate (32).

We identified a new assembly factor designated Mzm1 that also functions in the late stage of bc_1 biogenesis (1). Cells lacking Mzm1 exhibit a temperature-dependent defect in bc_1 maturation; ubiquinol-cytochrome *c* reductase activity is ~30% that of the wild type (WT) at 30°C and further reduced at 37°C. The mutant cells accumulate the late core assembly intermediate at both temperatures. Since the processing steps of Rip1 are unimpaired in *mzm1*Δ cells, we proposed that Mzm1 contributes to the late step of Rip1 maturation (2). In support of this model, we showed that the respiratory defect of *mzm1*Δ cells is efficiently bypassed by the overexpression of Rip1 and that Mzm1 transiently associates with Rip1 (2).

In the present study, we provide insight into the role of Mzm1 in the late phase of bc_1 maturation involving Rip1. We demonstrate that Mzm1 binds to the C-terminal globular domain of Rip1 and that residues at the extreme C terminus of Rip1 are important for this interaction. We demonstrate that Rip1 is prone to off-pathway misfolding at elevated temperatures in the absence of Mzm1, suggesting that Mzm1 chaperones Rip1 prior to Bcs1-mediated translocation. Whereas Mzm1 stabilization of Rip1 involves the C-terminal segment of Rip1, the N-terminal segment of Rip1 lacking the Rieske Fe/S domain is competent to induce stabilization of a nonfunctional bc_1:CcO supercomplex in *rip1*Δ cells. Interestingly, the permanent presence of Rip1 does not appear to be essential for the stability of this supercomplex; rather, the transient association of the Rip1 N terminus triggers stabilization of the supercomplexes.

MATERIALS AND METHODS

Yeast strains and vectors. Strains were BY4741 (*MAT***a** *his3*Δ*1 leu2*Δ*0 met15*Δ*0 ura3*Δ*0*). To generate *rip1*Δ strains, *RIP1* was replaced with the *kanMX6* coding sequence for selection. To generate *bcs1*Δ strains, *BCS1* was replaced with a *Candida albicans URA3* coding sequence. Except where specified, all cultures were grown at 30°C. Strains were grown in 2% galactose synthetic complete medium lacking relevant amino acids to maintain plasmid selection. For growth assays on solid media, synthetic complete medium was supplemented with relevant amino acids and 2% glucose, glycerol, or glycerol-lactate. Cultures for growth tests were grown in 2% glucose synthetic complete medium overnight and then normalized to an absorbance value at 600 nm of 1 and applied to solid medium in 1:10 serial dilutions.

Plasmids containing *MZM1* and *RIP1* were constructed as follows. *MZM1* was 3′ tagged with either Myc and six-histidine repeats or the FLAG epitope and placed under the control of the *MET25* promoter and the *CYC1* terminator on a pRS413 or pRS425 vector. On the pRS413 vector, DNA encoding the Sod2 mitochondrial targeting sequence (MTS) (amino acid residues 1 to 26) was added to target Mzm1 to the mitochondria, as the Sod2 MTS is a stronger signal than the endogenous MTS of Mzm1 (2). *RIP1* was cloned by PCR using primers anchored in the *RIP1* promoter and terminator appended with vector sequence to facilitate *in vivo* gap repair into BamHI- and NotI-digested pRS vector systems. This strategy created both pRS415 and pRS425 vectors bearing Rip1 under the control of its endogenous promoter and terminator. Using these *RIP1* plasmids as templates, plasmids containing the Myc (pRS425) and 3HA (pRS415) tags were generated by overlap extension PCR utilizing primers encoding the epitope tag together with vector-based primers. Additional Rip1 deletion constructs were generated using pRS425 Rip1-Myc as a template and 5′-phosphorylated primers to produce a linear vector product amenable to recircularization by ligation with Quick T4 ligase (New England BioLabs). The Rip1 extreme C-terminal truncations (Δ1, Δ4, and Δ6) were also generated by the same strategy using pRS315 Rip1 as a template. A pRS425 Mzm1-FLAG plasmid was similarly generated with phosphorylated primers by deleting the Myc and hexa-histidine epitopes while simultaneously adding the FLAG epitope. To ensure that the globular Rip1 construct is correctly targeted to the mitochondrial matrix, the Sod2 mitochondrial targeting sequence corresponding to amino acids 1 to 26 was cloned into a pRS413 vector containing the *MET25* promoter and *CYC1* terminator as an XbaI/BamHI fragment. The *RIP1* sequences corresponding to the C-terminal amino acid residues 81 to 215 and the Myc epitope were appended following the BamHI site using overlapping oligonucleotides and *in vivo* gap repair. The use of the Sod2 MTS and the *MET25* promoter resulted in very high Rip1 expression levels; therefore, the low-copy-number plasmid pRS413 was chosen to avoid overexpression. To generate the Rip1-Grx3 fusion plasmids, a plasmid template was used to amplify the glutaredoxin domain of Grx3 (codons 159 to 285) containing a C211S mutation that impairs Grx3 function. The oligonucleotides for amplification included Rip1 sequence homology such that *in vivo* ligation by gap repair into pRS425 Rip1-Myc generated constructs with 0, 20, or 30 C-terminal Rip1 residues (generating fusion proteins designated Grx3-0, Grx3-20, and Grx3-30, respectively [Fig. 6A]). All vectors were confirmed by sequencing at the University of Utah Core Facilities.

Preparation of mitochondria. Mitochondria were isolated as described previously (10). Briefly, lyticase was used to create spheroplasts, which were subsequently ruptured by Dounce homogenization, and mitochondria were isolated by differential centrifugation. The total mitochondrial protein concentration was estimated using the Bradford method.

SDS- and blue native-PAGE analysis. For SDS-PAGE, 10 to 30 μg of protein samples or mitochondria was separated on 12%, 4 to 12%, or 15% polyacrylamide gels and transferred to nitrocellulose or polyvinylidene difluoride (PVDF) membranes. Membranes were blocked prior to detection using 5 to 10% nonfat dry milk in phosphate-buffered saline (PBS) with or without 0.01% Tween 20. Blue native-PAGE (BN-PAGE) was performed essentially as described previously (29) or using a Bis-Tris system (Invitrogen) with either 1% digitonin or 1% dodecyl maltoside. Either chemiluminescent reagents with horseradish peroxidase-conjugated secondary antibodies or infrared (IR) dye-conjugated secondary antibodies (LI-COR) were used to visualize proteins. Antibodies were either purchased or generous gifts: anti-Myc (Roche Diagnostics), antiporin (Molecular Probes), anti-TAP (Open Biosystems), Cox1 (Mitosciences), anti-Rip1 and anti-Cor1/Cor2 (B. Trumpower), anti-Qcr10 (V. Zara), anti-Cox13 (P. Rehling), anti-Cyt1 (B. Meunier), and anti-F_1 ATPase beta subunit Atp2 (A. Tzagoloff).

Immunoprecipitation of Mzm1 and Rip1. Cells expressing Rip1 and Mzm1 constructs were grown on synthetic galactose medium with auxotrophic selection, and mitochondria were isolated as described above. Mitochondria (1 mg/ml protein) were lysed at 4°C in lysis buffer (20 mM Tris, pH 7.4, 100 mM NaCl, 1 mM phenylmethylsulfonyl fluoride [PMSF], Roche protease inhibitor cocktail, 2% digitonin, 0.5 mM EDTA, and 10% glycerol) and clarified by centrifugation at 20,000 × *g* for 15 min. Solubilized mitochondrial proteins were incubated with either Myc- or FLAG-conjugated agarose beads overnight at 4°C and then washed with 60 column volumes of wash buffer (20 mM Tris, pH 7.4, 100 mM NaCl, 1 mM PMSF, Roche protease inhibitor cocktail, 0.3% digitonin, 0.5 mM EDTA, and 10% glycerol). Bound proteins were eluted by the addition of either Myc or FLAG peptides.

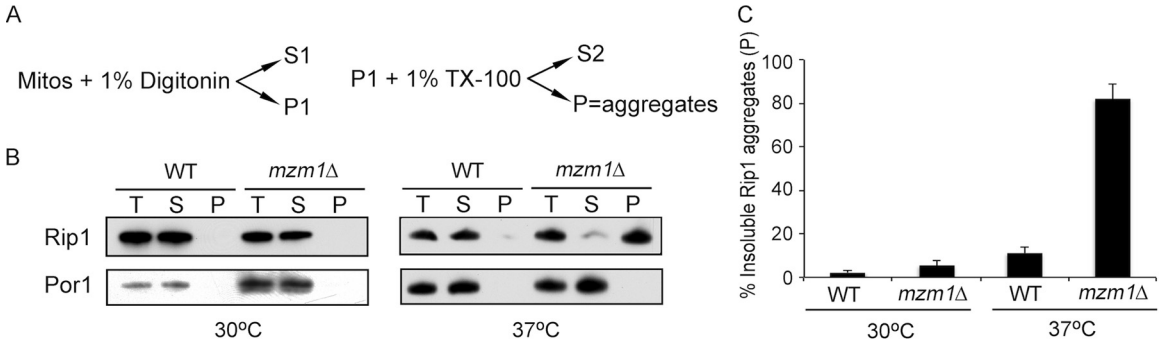

FIG 1 Rip1 aggregates at 37°C in the absence of Mzm1. (A) Schematic of the detergent-based protein aggregation assay; see Materials and Methods for details. (B) The total mitochondrial load (T), combined S1 and S2 soluble fractions (S), and insoluble material (P) were analyzed by SDS-PAGE and immunoblotting. At 30°C, the total load and the analyzed sample were 3-fold higher in concentration in *mzm1*Δ compared to WT, to produce samples with equivalent total Rip1 levels. (C) Comparison of the amount of Rip1 present by immunoblotting in the P fraction as a percentage of the total Rip1 protein (T), measured by ImageJ in three or more independent experiments.

Aggregation assay. Mitochondria were solubilized with digitonin lysis buffer (1% digitonin, 30 mM Tris, pH 7.4, 200 mM KCl, 5 mM EDTA, 0.5 mM PMSF, Roche protease inhibitor cocktail) for 30 min on ice. After centrifugation at 4°C for 30 min at 100,000 × *g*, the supernatant (solubilized fraction S1) was transferred to a new tube. The insoluble material of the pellet was then solubilized in Triton X-100 lysis buffer (1% Triton X-100, 30 mM Tris, pH 7.4, 200 mM KCl, 5 mM EDTA, 0.5 mM PMSF, Roche protease inhibitor cocktail) for 5 min, and the aggregated fraction (P) was separated from the supernatant (soluble fraction S2) by a second centrifugation at 4°C for 30 min at 100,000 × *g*. TCA-precipitated detergent-solubilized materials (S1 plus S2) were combined as the final soluble protein fraction (S). Both S and P fractions were solubilized in Laemmli buffer; additionally, a total (T) aliquot representing the total mitochondrial protein was not subjected to the aggregation assay but was solubilized in Laemmli buffer and included in the final SDS-PAGE analysis.

Mitochondrial enzymatic activity assays. The complex III activity of isolated mitochondria was measured spectrophotometrically by supplying decyl-ubiquinol and cytochrome *c* and following the rate of reduction of cytochrome *c* (while inhibiting complex IV with 2 mM KCN). Decyl-ubiquinol was prepared as described previously (1). The activity assay was performed with 30 μM decyl-ubiquinol, 0.4 mg/ml cytochrome *c* (from horse heart; Sigma-Aldrich), and 10 to 30 μg total mitochondrial protein in 40 mM potassium phosphate, pH 6.8, with 0.5% Tween 80. The initial rate of cytochrome *c* reduction at 550 nm was measured by an Agilent 8453 spectrophotometer.

RESULTS

Biological significance of Mzm1 interaction with Rip1. We previously reported that Mzm1 contributes to the late-step insertion of Rip1 into newly synthesized bc_1 (2). The translocation of Rip1 is impaired in *mzm1*Δ cells at the normal growth temperature for yeast (30°C), and this step is more substantially impaired under the stressful conditions of elevated temperature (37°C). To assess the state of the Rip1 protein in *mzm1*Δ mutant cells, a detergent-based protein aggregation assay was conducted. Centrifugation of mitochondria solubilized with digitonin generated a supernatant and pellet fraction. Reextraction of the pellet with Triton X-100 followed by ultracentrifugation yielded a pellet fraction consisting of detergent-insoluble material, including protein aggregates (Fig. 1A). Analyses of the supernatant and pellet fractions by immunoblotting revealed that Rip1 partitioned into the soluble fraction in WT and *mzm1*Δ cells at 30°C but was largely present in the particulate fraction at 37°C in *mzm1*Δ cells (Fig. 1B, lanes labeled P). Quantitation of the Rip1 partitioning in this experiment revealed that nearly 80% of the Rip1 present in *mzm1*Δ cells cultured at 37°C was particulate (Fig. 1C), likely due to protein aggregation.

This Rip1 aggregation was observed only in *mzm1*Δ cells cultured at elevated temperature. At 30°C, Rip1 in *mzm1*Δ was not significantly aggregated, but the steady-state level of Rip1 was significantly decreased, which was not the case at 37°C (compare the total levels of mitochondrial protein, represented by Por1, necessary to attain similar total loading of Rip1 in the aggregation assay) (Fig. 1B). Thus, in the absence of Mzm1, Rip1 is prone to proteolytic degradation or temperature-induced aggregation. Even an endogenous factor, such as the carbon source of the yeast growth medium, can affect whether Rip1 in *mzm1*Δ cells forms aggregates or is proteolytically degraded (here, galactose cultures at 37°C showed aggregated Rip1, whereas previously, glucose cultures propagated through the diauxic shift at 37°C showed marked attenuation in Rip1 steady-state levels [2]). It is clear that Mzm1 has a role in preventing those outcomes.

To assess the type of complex that forms between Mzm1 and Rip1, we used *bcs1*Δ cells in which Rip1 translocation is blocked, resulting in Rip1 retention within the mitochondrial matrix. Mitochondria isolated from *bcs1*Δ cells expressing Myc-epitope-tagged Mzm1 were solubilized with digitonin, and complexes were resolved via two-dimensional BN-PAGE (Fig. 2A to C). Mzm1 and Rip1 were evident in the low-mass region of the gel, and a fraction of Mzm1 and Rip1 comigrated. A fraction of Mzm1 was also found in a complex of slightly higher mass lacking Rip1. Immunoadsorption of Mzm1 by anti-Myc beads resulted in coprecipitation of Rip1 (Fig. 2D). This interaction between Mzm1 and Rip1 was abrogated in an Mzm1 mutant containing a Y11A substitution in the conserved N-terminal LYR motif (Fig. 2E). We previously reported that the Mzm1 Y11A point mutation results in a loss of Mzm1 function, as the mutant fails to support respiratory growth at 37°C (2).

Mapping the interaction interface on Rip1. To map the interaction interface between Mzm1 and Rip1, we initially constructed two C-terminal epitope-tagged Rip1 variants with Myc or hemagglutinin (3HA) appendages. Expression of these Rip1 variants in *rip1*Δ cells revealed that the Myc-tagged Rip1 construct was functional in conferring glycerol-lactate growth, whereas the 3HA variant failed to confer respiratory growth (Fig. 3A). The presence of either Rip1 epitope construct induced bc_1 activity in *rip1*Δ, but

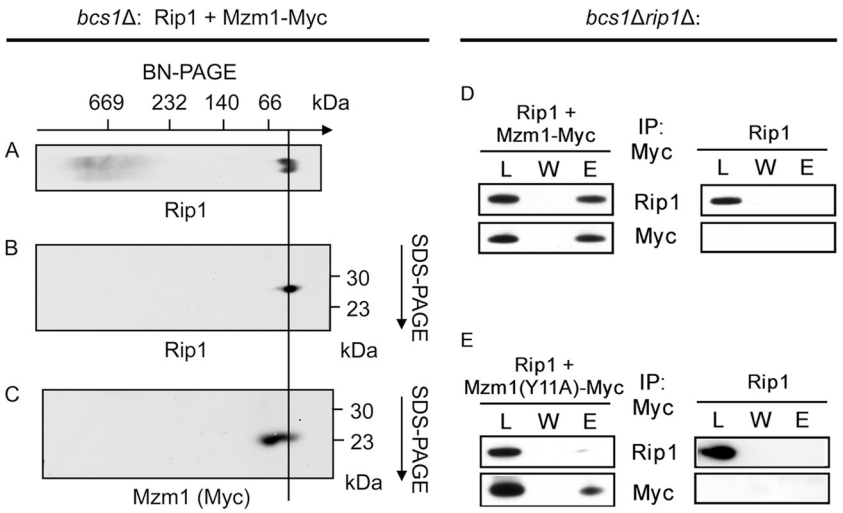

FIG 2 Rip1 and Mzm1 form a complex of low molecular mass, whose formation is dependent upon tyrosine-11 of Mzm1. (A) BN-PAGE analysis of mitochondria isolated from Δ*bcs1* cells expressing both YCp *RIP1* and YCp Sod2-*MZM1*-Myc, followed by immunoblot (anti-Rip1). (B and C) Subsequent analysis of the complex isolated through BN-PAGE by SDS-PAGE in a second dimension, followed by immunoblot (B, anti-Rip1; C, anti-Myc). The approximate positions of molecular masses are indicated, and a line is drawn as an aid to the eye indicating the Rip1-Mzm1 complex. (D and E) Immunoprecipitation of solubilized *bcs1*Δ *rip1*Δ mitochondria with anti-Myc antibody-conjugated agarose beads, showing the load (L), the final wash (W), and the eluate (E). Mitochondria were isolated from cultures expressing YCp *RIP1* and either YCp Sod2-*MZM1*-Myc (D) or YCp Sod2-*MZM1*-Myc with a mutation resulting in conversion of tyrosine-11 to alanine (E).

the activity in cells with Rip1-3HA was <25% of WT activity, a level insufficient to yield growth on glycerol-lactate medium. The steady-state level of the Rip1-3HA protein was markedly attenuated (Fig. 3B, lower panel), so the low catalytic activity likely stems from low Rip1 levels.

The bc_1 catalytic activity in *rip1*Δ cells with the Rip1-Myc variant remained substantial (Fig. 3B) and was sufficient to yield growth on glycerol-lactate medium (Fig. 3A). However, when the Rip1-Myc construct was expressed in WT cells containing the endogenous untagged Rip1, the endogenous Rip1 was preferentially incorporated into the bc_1 complex (as observed by BN-PAGE of digitonin-solubilized mitochondria) (Fig. 3C, compare lanes 2 and 3 to lanes 6 and 7 probed by anti-Myc antibody). Supercomplex formation was markedly attenuated in *rip1*Δ cells with the Rip1-3HA chimera, as expected from the reduced steady-state levels of this protein (Fig. 3C, lane 8). Supercomplex formation in

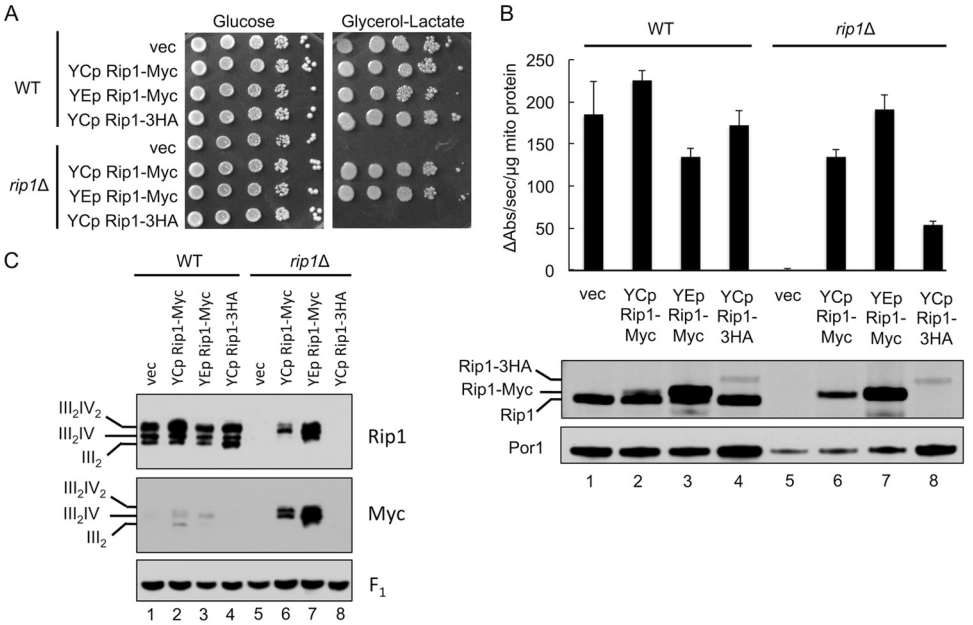

FIG 3 Rip1 is sensitive to C-terminal epitope tagging. (A and B) Growth assay at 30°C (A) as well as bc_1 complex activity assay and SDS-PAGE immunoblot of isolated mitochondria (B), from WT and *rip1*Δ cultures expressing vector control (vec) or YEp or YCp *RIP1*-Myc or YCp *RIP1*-3HA plasmid. (C) BN-PAGE immunoblot of digitonin-solubilized mitochondria isolated from the same cultures as in panels A and B.

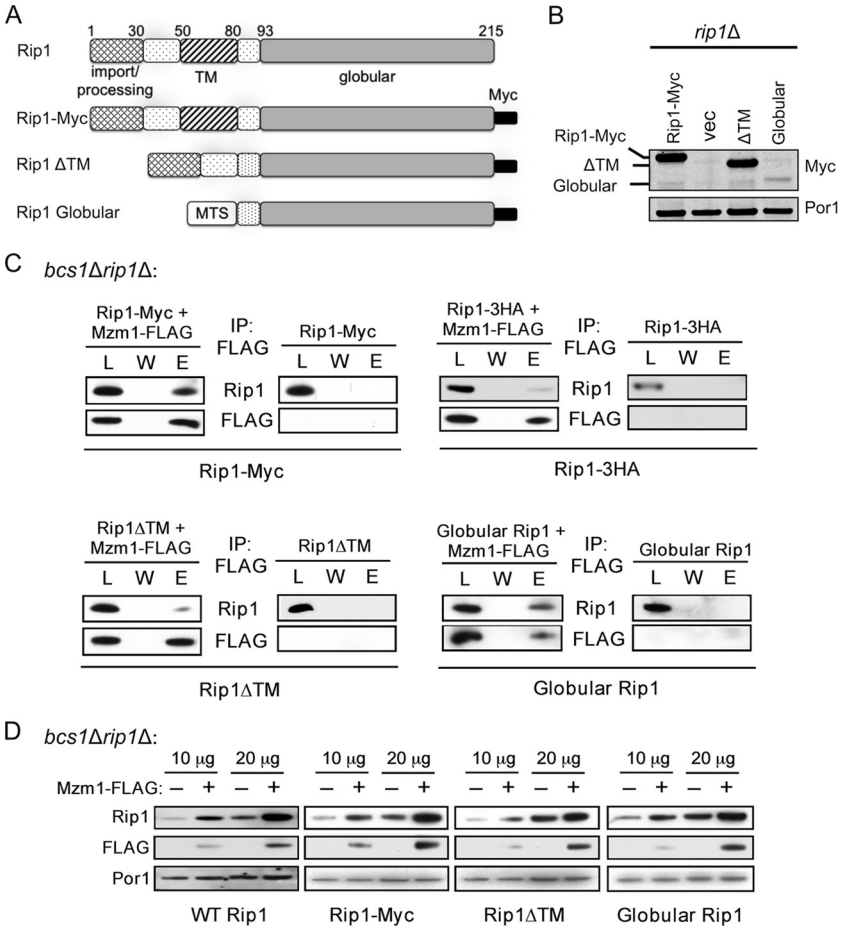

FIG 4 Mzm1 interacts with the C-terminal globular domain of Rip1. (A) Comparison of Rip1 domains present in the WT protein (prior to N-terminal processing), Rip1-Myc, and the ΔTM and globular Rip1 proteins, which lack residues 55 to 78 and 1 to 80, respectively. The globular Rip1 protein is targeted to the mitochondrial matrix by the mitochondrial targeting sequence of Sod2 (MTS) and expressed from a YCp plasmid; the other Rip1 variants contain the endogenous targeting region of Rip1 and were expressed from YEp plasmids. (B) SDS-PAGE immunoblot showing expression of these Rip1 variants in *rip1*Δ mitochondria. Vec, vector. (C) Immunoprecipitation of solubilized *bcs1*Δ *rip1*Δ mitochondria expressing these plasmids with anti-FLAG antibody-conjugated agarose beads, showing the total load (L), the final wash (W), and the eluate (E). The globular Rip1 protein was detected with anti-Myc antibody; all other Rip1 detections utilized anti-Rip1 antibody. (D) SDS-PAGE immunoblot of *bcs1*Δ *rip1*Δ mitochondria (10 and 20 μg total mitochondrial protein) expressing the Rip1 variant proteins in the presence and absence of YEp *MZM1*-FLAG.

*rip1*Δ cells overexpressing Rip1-Myc appeared normal, while cells expressing low-copy-number Rip1-Myc exhibited a slight diminution in supercomplex formation. Thus, the addition of a C-terminal tag on Rip1 has a deleterious effect on its function and, in the case of the 3HA appendage, also impairs its stability.

The Rip1-Myc variant exhibited an interaction with Mzm1. When this construct was expressed in *bcs1*Δ *rip1*Δ cells in the presence of FLAG-tagged Mzm1 for coimmunoprecipitation (co-IP) studies, immunoadsorption of Mzm1-FLAG resulted in copurification of Rip1-Myc (Fig. 4C). In contrast, adsorption of Mzm1-FLAG in cells harboring the Rip1-3HA chimera resulted in only weak co-IP of Rip1, which demonstrates the deleterious effect of this C-terminal 3HA tag on Rip1 function. Rip1 tagged by the single Myc epitope retained sufficient Rip1 function to permit its use in the construction of Rip1 truncations in the next series of studies.

Two Rip1 truncations were engineered to map the interaction interface for Mzm1. Yeast Rip1 consists of a 22-residue N-terminal mitochondrial target sequence (MTS) and an 8-residue Oct1 proteolytic processing motif, followed by a 62-residue segment containing a transmembrane (TM) helix motif and finally a globular domain containing the 2Fe-2S cluster (Fig. 4A). Rip1 constructs were engineered that lacked the TM motif or contained only the C-terminal 2Fe-2S-containing globular domain with a heterologous MTS. Immunoprecipitation of Mzm1-FLAG from *bcs1*Δ *rip1*Δ cells containing the Myc-tagged Rip1 truncations revealed an efficient coprecipitation of the Rip1 variant consisting of only the C-terminal globular domain (Fig. 4C). The Rip1 variant lacking the TM motif was attenuated in its interaction with Mzm1.

To corroborate the Rip1-Mzm1 interaction, we employed a Rip1 stabilization assay we used previously to document that overexpression of Mzm1 resulted in the enhanced stabilization of Rip1 in cells lacking Bcs1 (2). Expression of the Rip1 truncations in *bcs1*Δ *rip1*Δ cells in the presence and absence of a high-copy-number YEp vector expressing Mzm1-FLAG showed that overexpression of Mzm1 enhanced the stability of WT Rip1, Rip1-Myc, and Rip1 variants lacking the TM or containing only the globular domain (Fig. 4D). Additionally, overexpression of Mzm1 stabi-

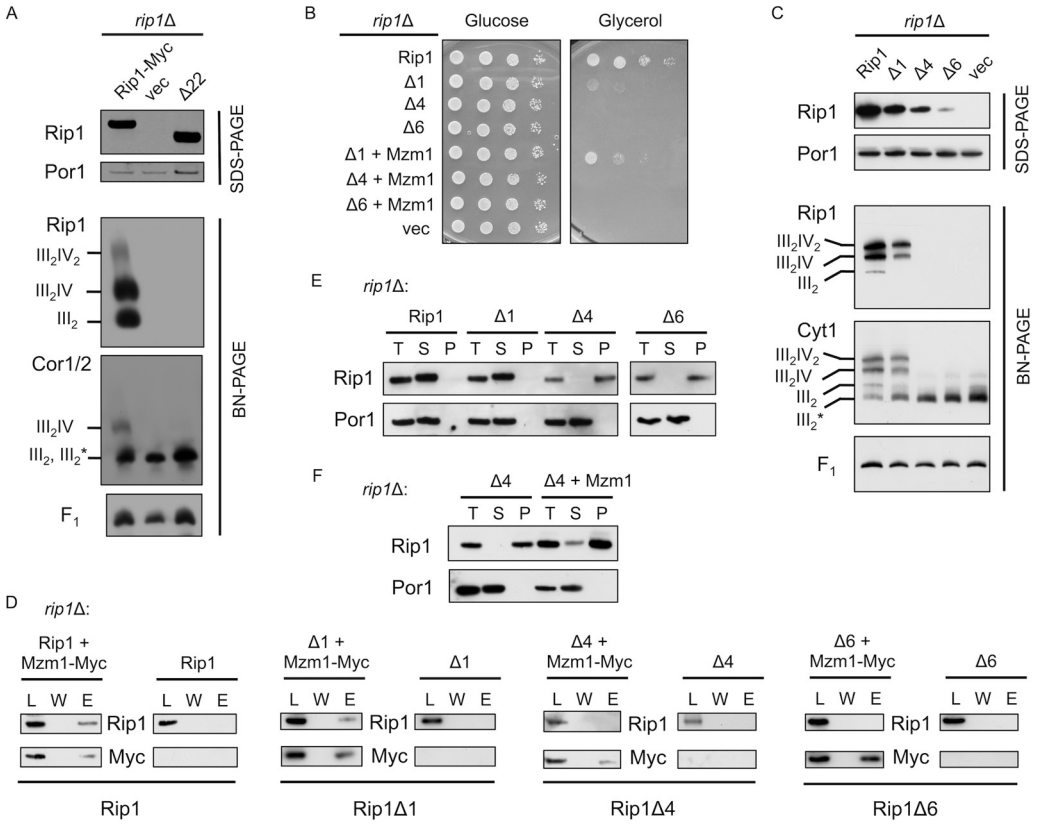

FIG 5 The extreme C terminus of Rip1 is essential for its function and important for interaction with Mzm1. (A) SDS-PAGE and BN-PAGE (digitonin) immunoblots of isolated mitochondria from WT and *rip1*Δ cultures expressing YEp *RIP1*-Myc, vector control (vec), or *rip1*Δ22 plasmid. Note that on this BN gel the dimeric bc_1 and late core intermediate comigrate, so the band designation includes both III_2 and III_2*, the latter of which denotes the late core intermediate formed during bc_1 complex assembly. The component is clearly the late core intermediate in the vector control *rip1*Δ cells. (B) Growth assay at 37°C of *rip1*Δ cultures expressing YCp *RIP1*, vector control, or the Δ1, Δ4, or Δ6 Rip1 truncation and coexpressing YCp vector control or *MZM1*-Myc plasmid. (C) SDS-PAGE and BN-PAGE (digitonin) immunoblots of *rip1*Δ cultures expressing YCp *RIP1*, Δ1, Δ4, Δ6, or vector control plasmid. (D) Immunoprecipitation of solubilized mitochondria from *rip1*Δ cultures expressing the plasmids listed in panel C with or without coexpression of YCp *MZM1*-Myc, using anti-Myc antibody-conjugated agarose beads and showing the total load (L), the final wash (W), and the eluate (E). (E) Detergent-based protein aggregation assay and SDS-PAGE immunoblot of the total load (T), soluble fraction (S), and pellet fraction (P), as described for Fig. 2 except that cultures were grown at 30°C with mitochondria isolated from *rip1*Δ cultures expressing the same plasmids as in panel C. The exposure of the Rip1Δ6 blot was extended due to limited steady-state levels of this truncation. (F) Assay described in E for a *rip1*Δ culture expressing the Δ4 truncation, with and without coexpression of YCp *MZM1*-Myc.

lized the Rip1-3HA fusion, although elevated levels of mitochondrial protein were needed to visualize this stabilization (not shown). The combination of the co-IP and Rip1 stabilization results confirms that Mzm1 interacts with the C-terminal globular domain of Rip1.

Mzm1 interaction with Rip1 C-terminal segment. To further refine the interaction interface, we constructed truncations of the Rip1 globular domain. We focused on the extreme C-terminal segment because we observed that C-terminal epitope tags (Myc and 3HA, as discussed above) altered the function of Rip1. The initial Rip1 C-terminal truncation that was constructed lacked the C-terminal 22 residues. Expression of this Rip1-Δ22 construct from a YEp vector in *rip1*Δ cells failed to support any respiratory growth. The truncation was stably expressed (Fig. 5A, SDS-PAGE blot), but the protein failed to be inserted into the bc_1 complex (Fig. 5A, anti-Rip1 BN-PAGE blot). In addition, no interaction was observed between Mzm1 and the Rip1 truncation by co-IP (data not shown).

A series of shorter C-terminal Rip1 truncations were engineered that lack 1, 4, or 6 C-terminal residues, and these constructs were expressed from low-copy-number YCp vectors in *rip1*Δ cells to assess their function. While cells harboring the WT Rip1 propagated well on glycerol growth medium, cells containing the Δ1, Δ4, and Δ6 variants were compromised in growth at 37°C (Fig. 5B), although cells containing the Rip1-Δ1 protein grew normally at 30°C (data not shown). These results are consistent with a recently published study of Rip1 truncations by Wagener et al. (27). Overexpression of Mzm1 restored partial 37°C glycerol growth in cells containing the Rip1-Δ1 deletion but not the Δ4 or Δ6 construct (Fig. 5B). The C-terminal truncations destabilized Rip1 in a length-dependent manner (Fig. 5C, SDS-PAGE panel). Consistent with this result and with the impaired respiratory growth at 37°C, mitochondria from Rip1-Δ4 and Rip1-Δ6 variants failed to show any Rip1 incorporation into the bc_1 complex at 30°C, and the late core assembly intermediate persisted in these cells as visualized by anti-Cyt1 immunoblotting (Fig. 5C, BN-PAGE panels).

Interaction studies were carried out to determine whether Mzm1 formed complexes with these impaired Rip1 truncations. As shown in Fig. 5D, immunoadsorption of Mzm1 led to the co-IP

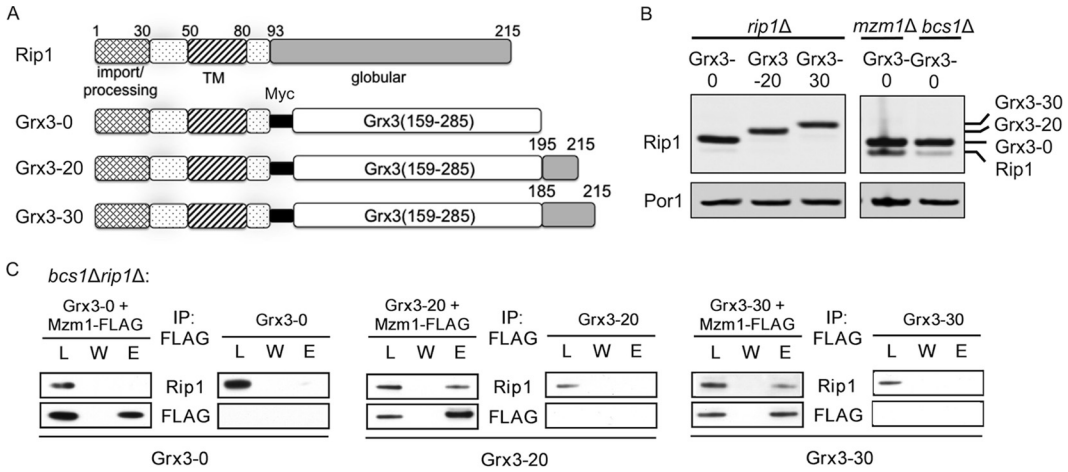

FIG 6 The C terminus of Rip1 is the dominant site for interaction with Mzm1. (A) Comparison of Rip1 domains present in the WT protein (prior to N-terminal processing) and the Grx3-0, Grx3-20, and Grx3-30 fusion proteins. These proteins are fusions of the N terminus of Rip1 (amino acid residues 1 to 92) with the soluble domain of Grx3 (residues 159 to 285), and each protein includes a Myc epitope positioned between the two domains. At the C terminus, 0, 20, or 30 residues of the Rip1 C terminus are appended. Note that these residues do not include any liganding residues for the 2Fe-2S center. (B) SDS-PAGE immunoblot of crude mitochondrial fractions showing expression of these fusion proteins from YEp plasmids. (C) Immunoprecipitation of solubilized *bcs1*Δ *rip1*Δ mitochondria expressing the fusion proteins from YEp plasmids, using anti-FLAG antibody-conjugated agarose beads and showing the total load (L), the final wash (W), and the eluate (E).

of Rip1 and Rip1-Δ1 but not the Rip1-Δ4 or Rip1-Δ6 protein. In the absence of an apparent interaction between Mzm1 and the Δ4 or Δ6 Rip1 truncation, we addressed whether those Rip1 proteins retained solubility by quantifying the detergent-insoluble fraction of each truncation in cells grown at 30°C (Fig. 5E). Rip1 truncations lacking either 4 or 6 C-terminal residues showed predominantly detergent-insoluble protein, in contrast to WT and the Δ1 variant, which were detergent soluble. However, in cells containing the Rip1-Δ4 truncation, overexpression of Mzm1 restored partial solubility of the truncation (Fig. 5F).

To validate a candidate Mzm1 interaction with the Rip1 C-terminal segment, a construct was generated in which the Rip1 globular domain was replaced with a similarly sized heterologous globular domain. The monothiol glutaredoxin domain of the yeast cytoplasmic Grx3 protein was used for this purpose. To minimize any deleterious effect of the presence of the glutaredoxin domain on mitochondrial redox balance, a C211A substitution was made to impair function. Two additional Rip1-Grx3 constructs were engineered in which either the C-terminal 20 or C-terminal 30 residues of Rip1 were appended to the Grx3 C terminus (Fig. 6A). The Rip1-Grx3 constructs expressed in *rip1*Δ cells were found to stably accumulate in mitochondria, and the Rip1-Grx3 protein lacking a Rip1 C-terminal appendage (labeled Grx3-0) accumulated in excess of endogenous Rip1 in *mzm1*Δ or *bcs1*Δ cells (Fig. 6B).

Studies to probe the interaction of Mzm1 and the Rip1-Grx3 chimeras were conducted in *rip1*Δ *bcs1*Δ cells. The Mzm1-mediated Rip1 stabilization assay (described above) showed no apparent stabilization of Rip1-Grx3 lacking any C-terminal Rip1 sequence (Grx3-0), but stabilization of the chimera containing 20 C-terminal Rip1 residues (Grx3-20) was reproducibly observed (data not shown). In support of this stabilizing interaction, co-IP studies showed a clear interaction of Mzm1 with the Rip1-Grx3 chimeras containing either 20 or 30 C-terminal Rip1 residues (Grx3-20 and Grx3-30) but not with the Rip1-Grx3 chimera lacking any additional C-terminal Rip1 residues (Grx3-0) (Fig. 6C). These results demonstrate that Mzm1 interacts with the C-terminal segment of Rip1.

Bcs1-mediated translocation of Rip1 variants. We next sought to identify the segment of Rip1 required for Bcs1-mediated translocation, initially by testing the Rip1 truncations described in Fig. 4A. We assessed whether expression of any of the Rip1 variants in *rip1*Δ cells would support formation of the bc_1:CcO supercomplex. Cells lacking Rip1 are stalled in assembly and accumulate a late core bc_1 intermediate deficient in both Rip1 and Qcr10 (7, 9, 31). This intermediate is seen in Fig. 7A (labeled III_2*). Expression of the Rip1-Grx3-0 and Rip1-Grx3-30 chimeras induced the formation of supercomplexes containing CcO as seen by BN-PAGE (shown by Cox2 immunoblotting in Fig. 7A). In contrast, expression of Rip1 lacking its TM or containing only the C-terminal globular domain failed to induce supercomplex formation. In the supercomplex formation induced by the Rip1-Grx3 chimeras, the chimeras were not visible by one-dimensional BN-PAGE (Fig. 7A), but trace levels of the chimeras were detected in the second SDS dimension shown in Fig. 7B (where Rip1 and the Rip1-Grx3 chimeras were exposed for equivalent times [anti-Myc panels]). Immunoblotting revealed that the supercomplex induced by Rip1-Grx3-0 contained Qcr10 (Fig. 7C), the last subunit added to yield the mature bc_1 complex, as well as Cox13, a late subunit of CcO assembly.

We carried out additional studies to address the requirements for supercomplex stabilization. First, we tested the dependency of the supercomplex formation on Bcs1; in the absence of Bcs1, no bc_1:CcO supercomplexes were formed (Fig. 7D). Second, we tested whether a C-terminal globular domain was necessary for Rip1-induced supercomplex formation/stabilization. We generated a Rip1 construct containing only the N-terminal 92 residues. Expression of this truncation (labeled 1-92) in *rip1*Δ cells restored the formation of supercomplexes containing Qcr10 and Cox13 (Fig. 7C). No Rip1 was apparent in the supercomplex, although the truncation was stably expressed. Thus, while the entire Rip1 molecule is obviously required for a functional supercomplex,

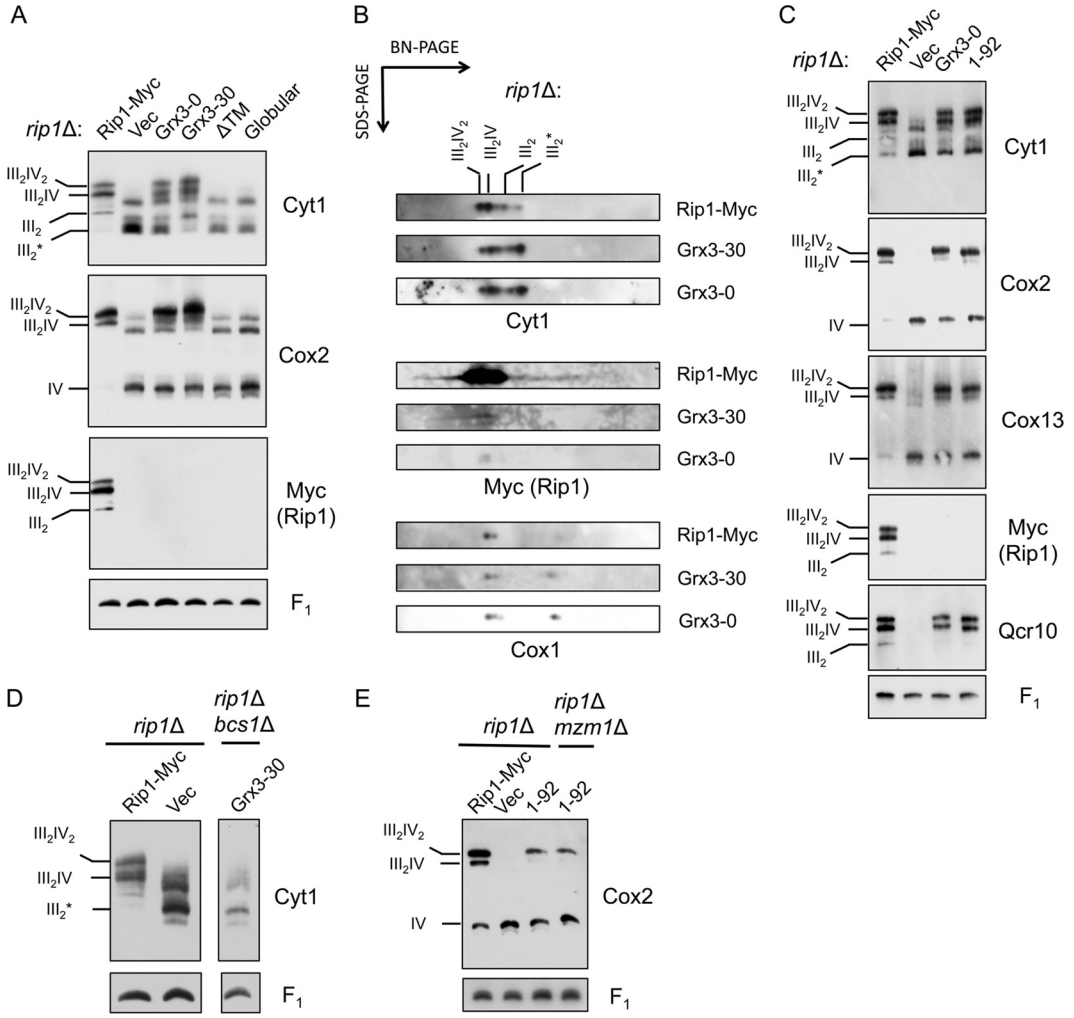

FIG 7 N-terminal Rip1 induces Bcs1-mediated bc_1:CcO supercomplex formation. (A) BN-PAGE (digitonin) immunoblots of isolated *rip1*Δ mitochondria expressing Rip1-Myc, vector (Vec), Grx3-0, Grx3-30, and Rip1 variants either lacking the TM domain (ΔTM) or only containing the C-terminal globular domain (Globular). All the constructs contain a Myc tag. All the constructs are expressed from YEp vectors except globular Rip1, which is expressed from a YCp vector. III_2* denotes the late core intermediate formed during bc_1 complex assembly. (B) Subsequent analysis of protein complexes isolated from *rip1*Δ mitochondria expressing Rip1-Myc, Grx3-0, or Grx3-30 through BN-PAGE by SDS-PAGE in a second dimension. (C) BN-PAGE (digitonin) immunoblots of isolated *rip1*Δ mitochondria expressing Rip1-Myc, vector, Grx3-0, or a Rip1 variant containing only the first 92 amino acid residues (1-92) with a C-terminal Myc tag. (D) BN-PAGE (digitonin) immunoblots of isolated *rip1*Δ mitochondria expressing Rip1-Myc or vector and *rip1*Δ *bcs1*Δ mitochondria expressing Grx3-30. (E) BN-PAGE (digitonin) immunoblots of isolated *rip1*Δ mitochondria expressing Rip1-Myc, vector, or the Rip1 (1-92) variant and *rip1*Δ *mzm1*Δ mitochondria expressing the Rip1 (1-92) variant. The Rip1 (1-92) variant is processed in the matrix, and the mature form consists of residues 31 to 92.

only the N terminus of Rip1 is necessary to induce supercomplex formation/stabilization. Third, we tested the dependency of the supercomplex stabilization on Mzm1 and found that the Rip1 truncation-induced supercomplex formation is independent of the presence of Mzm1 (Fig. 7E).

Previously, *rip1*Δ cells were reported to be deficient in bc_1:CcO supercomplexes when BN-PAGE was used as an assay, but a low-abundance complex containing a CcO subunit was observed at a lower mass than that of the usual supercomplexes (also seen as the unlabeled bands visible by anti-Cyt1 and anti-Cox2 immunoblotting in Fig. 7A, lane Vec) (8). This complex represents the late core assembly intermediate of bc_1 within supercomplexes with CcO, and these complexes are largely destabilized by BN-PAGE conditions (21). Using coimmunoprecipitation as an assay, the bc_1:CcO supercomplex was found to be as stable in *rip1*Δ as WT cells, unless Coomassie is added to the IP reaction (data not shown). Thus, the appearance of supercomplexes in *rip1*Δ when the Rip1-Grx3 chimeras and the Rip1 truncation are expressed (Fig. 7A and C) is due to the increased stability of the bc_1:CcO supercomplexes, which would otherwise be unstable under BN-PAGE conditions.

DISCUSSION

The final step in bc_1 biogenesis in yeast involves the insertion of the Rieske Fe/S protein Rip1, along with the Qcr10 subunit (7, 31). Rip1 is fully imported into the mitochondrial matrix compartment (16), and formation of the 2Fe-2S center likely occurs by the ISC Fe-S cluster system (18) prior to translocation across the IM by the Bcs1 ATPase. Bcs1 associates with the late core assembly intermediate and mediates Rip1 translocation in an ATP-dependent process (27). Cells lacking Bcs1 are stalled in bc_1 formation at

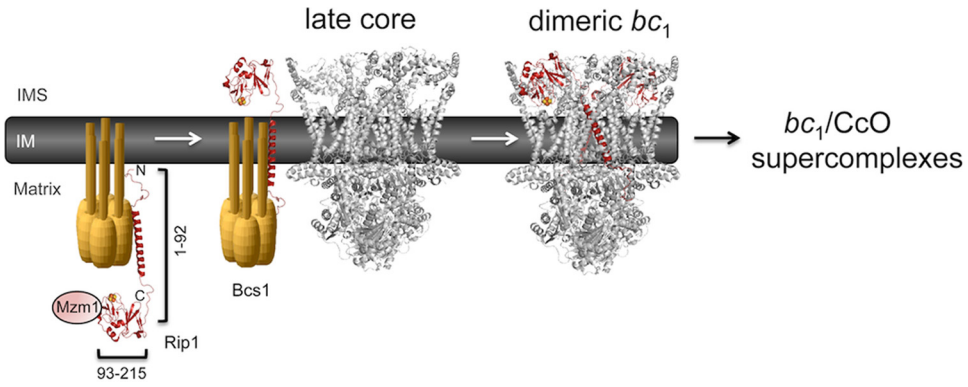

FIG 8 Model for the chaperone role of Mzm1 in stabilizing the C-terminal domain of Rip1. Mzm1 is shown to interact with and stabilize the C-terminal globular domain of Rip1 prior to translocation by Bcs1. The N-terminal half of Rip1 (residues 1 to 92) is shown to be functional in inducing stabilization of the bc_1:CcO supercomplex in *rip1*Δ cells.

the late core intermediate, and Rip1 remains an unstable protein within the matrix (27, 32).

We demonstrated previously that Mzm1 also functions at this late step of Rip1 maturation in bc_1 biogenesis (2). Here, we investigate the role of Mzm1 and define its interaction with Rip1. We have found that Mzm1 functions within the matrix as a Rip1 chaperone, forming a low-molecular-weight complex with Rip1 that is dependent on the tyrosine residue in the conserved LYR motif of Mzm1. This finding suggests a role for the tyrosine in this motif, without which Mzm1 is nonfunctional, in enabling Mzm1-Rip1 interaction. The resulting Mzm1-Rip1 complex serves to stabilize Rip1 prior to translocation by Bcs1. In the absence of this interaction, Rip1 is prone to either proteolytic degradation or aggregation.

Our analysis also indicates that Mzm1 associates with the C-terminal globular domain of Rip1. Replacing this globular domain with the heterologous folded domain of Grx3 to form a Rip1-Grx3 chimera abrogates the interaction with Mzm1. However, appending the C-terminal 20 residues of Rip1 to this Rip1-Grx3 chimera restores Mzm1 interaction. Thus, the C-terminal peptide segment of Rip1 is a dominant site for interaction with Mzm1 (see model in Fig. 8).

Formation of the 2Fe-2S cluster in Rip1 likely occurs within the matrix by the ISC Fe-S cluster biogenesis system prior to Bcs1-mediated translocation (19). Mzm1 may contribute to the stabilization of Rip1 independent of Fe-S cluster status. Fe-S cluster formation is also not a prerequisite for Bcs1-mediated insertion of Rip1 (2, 9, 15).

The C-terminal segment of Rip1 is a key determinant for Rip1 function and stability. Fusion of either a C-terminal Myc or 3HA epitope tag impairs function and, in the case of the 3HA fusion, markedly impairs stability. The Rip1-Myc fusion protein is stable and can be incorporated into the mature bc_1 complex, as well as bc_1:CcO supercomplexes. However, when that protein is expressed in WT cells, the cells preferentially incorporate the WT Rip1 rather than the Myc-tagged protein, despite its high expression level. The inefficient incorporation of the Myc-tagged protein is suggestive of a negative effect of the tag on the translocation step or on the release from Bcs1. In addition, removal of as few as four C-terminal Rip1 residues impairs the assembly process and results in a detergent-insoluble protein that is likely aggregated. This Δ4 C-terminal Rip1 truncation also fails to interact with Mzm1. Since the Δ4 Rip1 truncation is aggregated at 30°C, the prediction is that the truncation results in aggregation-prone protein independently of the loss of the Mzm1 interaction.

Insights into the Rip1 determinants necessary for Bcs1-mediated translocation also emerge from the present studies. Rip1 translocation is implied by the Rip1-induced stabilization of bc_1:CcO supercomplexes in a Bcs1-dependent manner. We find that this process requires only the N-terminal 92 residues of Rip1. The enhanced supercomplex stabilization induced by the 92-residue truncation lacking the C-terminal dominant site for interaction with Mzm1 suggests that Mzm1 may not have a significant role in Rip1 presentation to Bcs1 for translocation. In contrast, the C-terminal globular domain of Rip1 lacks the ability to stabilize bc_1:CcO supercomplexes. Thus, separate and distinct domains of Rip1 are responsible for its stabilization in the matrix by Mzm1 and its translocation into the IM by Bcs1. A model for the effect of Mzm1 on Rip1 is shown in Fig. 8.

*bc*1:CcO supercomplex stabilization induced by either the Rip1-Grx3 chimeras or the Rip1 truncation containing only the N-terminal 92 residues results in the incorporation of late subunits of each complex, Qcr10 and Cox13. However, the supercomplexes lack the Rip1 variants. The interface of the bc_1:CcO supercomplex is projected to be formed by Cob, Rip1, and Qcr10 of bc_1 and Cox9, Cox13, and Cox3 of CcO (12). Supercomplex formation is not impaired in cells lacking Qcr6, Qcr10, Cox8, Cox12, or Cox13 (21). The stability of the *bc*1:CcO supercomplex is dependent on cardiolipin (28), Aac2 (6, 11), and two additional recently identified proteins, Rcf1 and Rcf2 (5, 22, 26). The mechanism by which the Rip1 truncation induces supercomplex stabilization is unresolved. Several potential models are envisioned. First, translocation of the truncation may lead to transient association with the late core intermediate of bc_1, resulting in Qcr10 association and subsequent binding of CcO. This supercomplex may have sufficient stability that upon dissociation of the Rip1 truncation, the bc_1:CcO complex is retained. Second, Bcs1 may have an active role in the recruitment and insertion of Qcr10 (or a supercomplex-associated protein such as Rcf1) without the translocation of the Rip1 truncation. This mechanism might arise if Bcs1 had a remodeling function with the late core assembly intermediate. Future studies will focus on this step. The Rip1 truncation-induced supercomplex stabilization is independent of Mzm1

and the Rip1 C-terminal domain, whereas the TM domain of Rip1 is shown to be essential for this stabilization effect.

ACKNOWLEDGMENTS

This work was supported by grant GM083292 to D.R.W. P.M.S. was supported by training grant T32 DK007115. J.L.F. was supported by training grant T32 HL007576-25. O.K. was supported by American Heart Association fellowship 10POST4300044.

We thank Hyung Kim for helpful discussions.

REFERENCES

1. **Atkinson A, et al.** 2010. Mzm1 influences a labile pool of mitochondrial zinc important for respiratory function. J. Biol. Chem. **285**:19450–19459.
2. **Atkinson A, et al.** 2011. The LYR protein Mzm1 functions in the insertion of the Rieske Fe/S protein in yeast mitochondria. Mol. Cell. Biol. **31**:3988–3996.
3. **Bachmann J, Bauer B, Zwicker K, Ludwig B, Anderka O.** 2006. The Rieske protein from *Paracoccus denitrificans* is inserted into the cytoplasmic membrane by the twin-arginine translocase. FEBS J. **273**:4817–4830.
4. **Brandt U, Uribe S, Schagger H, Trumpower BL.** 1994. Isolation and characterization of *QCR10*, the nuclear gene encoding the 8.5-kDa subunit 10 of the *Saccharomyces cerevisiae* cytochrome bc_1 complex. J. Biol. Chem. **269**:12947–12953.
5. **Chen YC, et al.** 2012. Identification of a protein mediating respiratory supercomplex stability. Cell Metab. **15**:348–360.
6. **Claypool SM, Oktay Y, Boontheung P, Loo JA, Koehler CM.** 2008. Cardiolipin defines the interactome of the major ADP/ATP carrier protein of the mitochondrial inner membrane. J. Cell Biol. **182**:937–950.
7. **Crivellone MD, Wu MA, Tzagoloff A.** 1988. Assembly of the mitochondrial membrane system. Analysis of structural mutants of the yeast coenzyme QH_2-cytochrome *c* reductase complex. J. Biol. Chem. **263**:14323–14333.
8. **Cruciat CM, Brunner S, Baumann F, Neupert W, Stuart RA.** 2000. The cytochrome bc_1 and cytochrome *c* oxidase complexes associate to form a single supracomplex in yeast mitochondria. J. Biol. Chem. **275**:18093–18098.
9. **Cruciat CM, Hell K, Folsch H, Neupert W, Stuart RA.** 1999. Bcs1, an AAA-family member, is a chaperone for the assembly of the cytochrome bc_1 complex. EMBO J. **18**:5226–5233.
10. **Diekert K, De Kroon AI, Kispal G, Lill R.** 2001. Isolation and subfractionation of mitochondria from the yeast *Saccharomyces cerevisiae*. Methods Cell Biol. **65**:37–51.
11. **Dienhart MK, Stuart RA.** 2008. The yeast Aac2 protein exists in physical association with the cytochrome bc_1-COX supercomplex and the TIM23 machinery. Mol. Biol. Cell **19**:3934–3943.
12. **Dudkina NV, Kudryashev M, Stahlberg H, Boekema EJ.** 2011. Interaction of complexes I, III, and IV within the bovine respirasome by single particle cryoelectron tomography. Proc. Natl. Acad. Sci. U. S. A. **108**:15196–15200.
13. **Esser L, et al.** 2008. Inhibitor-complexed structures of the cytochrome bc_1 from the photosynthetic bacterium *Rhodobacter sphaeroides*. J. Biol. Chem. **283**:2846–2857.
14. **Golik P, Bonnefoy N, Szczepanek T, Saint-Georges Y, Lazowska J.** 2003. The Rieske FeS protein encoded and synthesized within mitochondria complements a deficiency in the nuclear gene. Proc. Natl. Acad. Sci. U. S. A. **100**:8844–8849.
15. **Graham LA, Trumpower BL.** 1991. Mutational analysis of the mitochondrial Rieske iron-sulfur protein of *Saccharomyces cerevisiae*. III. Import, protease processing, and assembly into the cytochrome bc_1 complex of iron-sulfur protein lacking the iron-sulfur cluster. J. Biol. Chem. **266**:22485–22492.
16. **Hartl FU, Schmidt B, Wachter E, Weiss H, Neupert W.** 1986. Transport into mitochondria and intramitochondrial sorting of the Fe/S protein of ubiquinol-cytochrome *c* reductase. Cell **47**:939–951.
17. **Iwata S, et al.** 1998. Complete structure of the 11-subunit bovine mitochondrial cytochrome bc_1 complex. Science **281**:64–71.
18. **Lill R, Muhlenhoff U.** 2008. Maturation of iron-sulfur proteins in eukaryotes: mechanisms, connected processes, and diseases. Annu. Rev. Biochem. **77**:669–700.
19. **Muhlenhoff U, Richter N, Pines O, Pierik AJ, Lill R.** 2011. Specialized function of yeast Isa1 and Isa2 proteins in the maturation of mitochondrial [4Fe-4S] proteins. J. Biol. Chem. **286**:41205–41216.
20. **Nett JH, Trumpower BL.** 1999. Intermediate length Rieske iron-sulfur protein is present and functionally active in the cytochrome bc_1 complex of *Saccharomyces cerevisiae*. J. Biol. Chem. **274**:9253–9257.
21. **Pfeiffer K, et al.** 2003. Cardiolipin stabilizes respiratory chain supercomplexes. J. Biol. Chem. **278**:52873–52880.
22. **Strogolova V, Furness A, Robb-McGrath M, Garlich J, Stuart RA.** 2012. Rcf1 and Rcf2, members of the hypoxia induced gene 1 protein family, are critical components of the mitochondrial cytochrome bc_1-cytochrome *c* oxidase supercomplex. Mol. Cell. Biol. **32**:1363–1373.
23. **Stuart RA.** 2008. Supercomplex organization of the oxidative phosphorylation enzymes in yeast mitochondria. J. Bioenerg. Biomembr. **40**:411–417.
24. **van Loon AP, Schatz G.** 1987. Transport of proteins to the mitochondrial intermembrane space: the 'sorting' domain of the cytochrome c_1 presequence is a stop-transfer sequence specific for the mitochondrial inner membrane. EMBO J. **6**:2441–2448.
25. **Vonck J, Schafer E.** 2009. Supramolecular organization of protein complexes in the mitochondrial inner membrane. Biochim. Biophys. Acta **1793**:117–124.
26. **Vukotic M, et al.** 2012. Rcf1 mediates cytochrome oxidase assembly and respirasome formation, revealing heterogeneity of the enzyme complex. Cell Metab. **15**:336–347.
27. **Wagener N, Ackermann M, Funes S, Neupert W.** 2011. A pathway of protein translocation in mitochondria mediated by the AAA-ATPase Bcs1. Mol. Cell **44**:191–202.
28. **Wenz T, et al.** 2009. Role of phospholipids in respiratory cytochrome bc_1 complex catalysis and supercomplex formation. Biochim. Biophys. Acta **1787**:609–616.
29. **Wittig I, Braun HP, Schagger H.** 2006. Blue native PAGE. Nat. Protoc. **1**:418–428.
30. **Xia D, et al.** 1997. Crystal structure of the cytochrome bc_1 complex from bovine heart mitochondria. Science **277**:60–66.
31. **Zara V, Conte L, Trumpower BL.** 2009. Evidence that the assembly of the yeast cytochrome bc_1 complex involves the formation of a large core structure in the inner mitochondrial membrane. FEBS J. **276**:1900–1914.
32. **Zara V, Conte L, Trumpower BL.** 2007. Identification and characterization of cytochrome bc_1 subcomplexes in mitochondria from yeast with single and double deletions of genes encoding cytochrome bc_1 subunits. FEBS J. **274**:4526–4539.